Università degli Studi di Genova
DIPTERIS – Cattedra di Geochimica

Università degli Studi di Firenze
Dipartimento di Scienze della Terra

Luigi Marini and Giulio Ottonello (Series Editors)
Antonella Buccianti, Luigi Marini, Giulio Ottonello and Orlando Vaselli (Eds.)

Proceedings of the Arezzo Seminar on Fluids Geochemistry

held in Arezzo on August 29th – September 1st, 2000
under the sponsorship of

Società Geochimica Italiana

International Association for Mathematical Geology

CNR – C.S. Minerogenesi e Geochimica Applicata di Firenze

PACINIeditore

FINITE ELEMENT MODELING OF GAS DISPERSION IN THE ATMOSPHERE

Giovanni Macedonio, Antonio Costa

Osservatorio Vesuviano, Via Diocleziano 328, I-80124 Napoli, Italy (e-mail: macedon@ov.ingv.it).

ABSTRACT

Gas emitted in the atmosphere are transported by the winds and are subject to turbulent diffusion. The dynamics of gas dispersion is described by the transport theory, which is based on a set of partial differential equations describing the balance of mass, momentum, and energy of the transported gas species. Although gases are compressible, they can be approximated as incompressible fluids whenever their velocity is small compared to the sound speed and the time scale of the velocity variations are greater than the travel time of the sound waves in the domain of interest. This condition is often verified for gas dispersion in the atmosphere, and allows us to neglect density variations in the mass balance equation. The small density inhomogeneities due to their differences in composition and temperature that are responsible for the convective motions are accounted for in the momentum equation (Boussinesq approximation). Turbulence poses the problem of the "closure of the equations", and further models are needed to describe the effects of the random turbulent fluctuations of velocity, pressure, *etc.* as a function of their mean values. Owing to the nonlinear character of the transport equations, numerical integration is often required to solve most of the practical problems. Both Finite Difference and Finite Element methods are used for spatial and temporal discretization, while time integration is based on either explicit (often unstable) or implicit schemes. Here, we will consider the Finite Element method, and a numerical example of gas dispersion in the atmosphere from a ground source is presented.

INTRODUCTION

In this paper a brief description of the theory underlying gas transport in the atmosphere is presented. We will focus our attention on the processes occurring in the lower part of the troposphere, in direct contact with the Earth surface: the so called "boundary layer". The boundary layer is directly influenced by the presence of the ground and responds to the surface forcing with a time scale of an hour or less (Stull, 1988). These forcing include frictional drag, evaporation and transpiration, heat transfer, pollutant emission, gas emission from the ground, formation of fog and clouds. A typical boundary layer thickness ranges between hundreds of meters to a few kilometers. The atmospheric temperature in the boundary layer shows diurnal variations. These are not due to direct heating of the lower atmosphere by the solar radiation, but to the heating and cooling of the ground in response to the adsorption of the radiation during the day, and re-emission during the night. The boundary layer, in turn, warms and cools via transport processes, mostly controlled by turbulence. The dynamics of the atmosphere in the boundary layer is described by the transport equations. These include the continuity equation (mass balance), and the momentum and energy balance equations. When pollutant gases are present, additional mass balance equations are needed for each gas specie. Under simple hypotheses (eg: steady state, simple topography, etc.) transport equations can be solved analytically; however, very often, these need to be solved numerically (Pasquill, 1974; Jacobson, 1999). In the latter case the differential equations, defined in the continuum, are spatially discretized using either the Finite Difference or the Finite Element Method, and are also integrated in time using different algorithms (implicit or explicit). Both techniques show their advantages and disadvantages. Usually Finite Differences allow faster computation, but are less suitable in the case of a complex shape of the computational domain. Here we will restrict to the description of the Finite Element Method.

TRANSPORT THEORY

The dynamics of fluids (air in our case) is described by the transport theory, which is based on the balance equations of mass, momentum and energy. In this section we will briefly describe these relations, whereas, in the following, a particular technique of solution based on the Finite Element Method will be presented. The balance equations are usually derived using the *Eulerian approach*. In this approach, a fixed control volume is used, and the fluid is described as it passes through that volume. As an example, the conservation of mass states that the temporal variation of the mass in that volume equals the total mass flux crossing its boundary surface. In the case of an infinitesimal control volume, we obtain the following equation of continuity (Bird et al., 1960; Landau & Lifchitz, 1971):

$$\frac{\partial \rho}{\partial t} + \nabla \cdot (\rho \mathrm{v}) = 0 \tag{1}$$

where ρ is the density of the fluid (air in our case), $\mathbf{v}$ is the fluid velocity, t is time and ∇ is the "nabla" operator (gradient). The first term of eq. (1) represents the rate of change of the mass with time in the infinitesimal control volume, whereas the second term, represents the mass flux passing through its boundaries.

For what concerns the dynamics of the lower atmosphere, air can be considered incompressible, provided that its velocity is much less than the corresponding sound velocity a ($a \approx 330$ m/s), and the condition $\tau_c >> L_c/a$ is fulfilled, where τ_c and L_c are the characteristic time and length scales of the velocity changes (Landau & Lifchitz, 1971; Monin & Yaglom, 1979). In this case, during the gas motion, the variations in density due to changes in the pressure are negligible and, following the Boussinesq approximation, changes in the density due to differences in temperature are accounted for only in the momentum balance equation. By setting ρ = const, eq. (1) reduces to:

$$\nabla \cdot \mathbf{v} = 0 \tag{2}$$

In a similar way as above, the Netwon's second law applied to an incompressible fluid passing through an infinitesimal, fixed control volume leads to the following momentum balance equation:

$$\rho \frac{\partial \mathbf{v}}{\partial t} + \rho \mathbf{v} \cdot \nabla \mathbf{v} = -\nabla P + \rho \mathbf{g} + \nabla \cdot \tau \tag{3}$$

where $\mathbf{g}$ is the gravity acceleration, P is the pressure, and $\boldsymbol{\tau}$ is the shear stress tensor that accounts for the viscous friction. The first term in the left represents the rate of change of momentum in the control volume per unit time and is null in the steady-state regime. The following advective term accounts for the transport of momentum by the fluid and represents the "inertial" forces; this term is non-linear, and is responsible of the fluid turbulence (at high Reynolds numbers). The terms on the right represent respectively the force acting on the fluid due to pressure gradients, the body forces (eg: gravity), and the viscous forces. Fluids that are characterized by a strain rate proportional to the applied shear stress (eg: air), are called *Newtonian*; in this case the stress tensor may be written as:

$$\tau = \mu(\nabla \boldsymbol{v} + \nabla \boldsymbol{v}^{T}) \tag{4}$$

where μ is the (dynamic) viscosity coefficient, and the superscript ^{T} represents the transpose operator. The stress tensor τ is symmetric, with null trace, thanks to the continuity equation (2). When the temperature cannot be considered constant, the above equations are coupled with the following energy balance equation, also valid for incompressible fluids:

$$\rho c_p \left(\frac{\partial T}{\partial t} + \mathbf{v} \cdot \nabla T \right) = \nabla \cdot (k \nabla T) + \tau \cdot \nabla \mathbf{v} \tag{5}$$

where c_p is the heat capacity at constant pressure, and k is the thermal conductivity. The term on the left represents the temporal variation of the enthalpy along the streamline passing through the infinitesimal control volume, whereas the terms on the right represent respectively the heat exchange by conduction and heat generation by viscous friction. This last term is usually negligible in atmospheric processes.

Equations (2), (3) and (5) represent a set of five equations in the five unknowns v_x, v_y, v_z, (the three compo-

nents of the velocity), P, and T. These can be integrated in a given physical domain, once the proper initial and boundary conditions are set, and gas density and viscosity are known. As will be seen later, however, the presence of turbulence does not allow a direct integration of the above equations, and additional equations are needed to "close" the system of equations.

Transport of pollutants in the atmosphere

Pollutants transport in the atmosphere is described by the following mass balance equation:

$$\frac{\partial C}{\partial t} + \nabla \cdot (C\mathbf{v}) = \nabla \cdot (D\nabla C) \tag{6}$$

where C represents the gas concentration of the pollutant gas (eg: mass per unit volume). The first term describes the temporal variation of C in the infinitesimal volume, whereas the following advective term describes the gas transport by the carrier fluid (air), moving at velocity $\mathbf{v} \equiv (v_x, v_y, v_z)$. This equation results from balancing the temporal variation of C with the gas fluxes exiting from the control volume, in the same way as for equation (1). The term at the second side represents the gas flux due to molecular diffusion, where D is the diffusion coefficient. As can be noted, even when the gas velocity is null, gas concentration may vary due to molecular diffusion. The molecular diffusion coefficient D is a function of the molecular weight and increases with temperature. Typical values are of the order of 10^{-5} m^2/s. However, in the atmosphere, air flow is often turbulent, allowing more efficient diffusion and mixing. In this case molecular diffusion can be neglected compared with turbulent diffusion which is greater than the former by several orders of magnitude.

Boundary conditions

To solve the transport equations, boundary conditions must be specified for the velocity $\mathbf{v}$, the temperature T, the pressure P, and components concentration C. Alternatively, prescribed values of the stress tensor $\boldsymbol{\tau}$ and pressure P, and/or heat and components fluxes may be present. In the former case we have:

$$v_i = v_{0i} \quad \text{on} \quad \Gamma_v \tag{7}$$

where v_{0i} is the prescribed value of the component i of the velocity on the external surface Γ_v of our volume of interest. If stresses are prescribed at the boundary:

$$\sigma_{ij} n_j = \sigma_{0i} \quad \text{on} \quad \Gamma_\sigma \tag{8}$$

where n_j are the components of the versor normal to the boundary surface, and σ_{0i} are the prescribed stresses including both normal stress (pressure) and shear stress:

$$\sigma_{ij} = -P\delta_{ij} + \tau_{ij} \tag{9}$$

The Kronecker symbol δ_{ij} represents the components of the identity matrix:

$$\delta_{i,j} = \begin{cases} 1 & i = j \\ 0 & i \neq j \end{cases} \tag{10}$$

We assume that the two portions of the boundary surface Γ_v and Γ_σ are such that:

$$\Gamma_v \cup \Gamma_\sigma = \Gamma \quad \text{(the whole boundary surface)} \tag{11}$$

$$\Gamma_v \cap \Gamma_\sigma = \theta \quad \text{(the empty set)} \tag{12}$$

Usually, conditions of the former type (on Γ_v) apply to the inlet (or outlet) or to no-slip boundaries, whereas the boundary condition of the latter type (on Γ_σ) apply to the slip boundaries (eg: the free surface, symmetry planes, etc.).

In a similar way as above, the boundary conditions for the temperature T are of two kinds: those with prescribed temperatures, and those with prescribed heat fluxes. In the former case we have:

$$T = T_0 \quad \text{on} \quad \Gamma_T \tag{13}$$

where T_0 is the prescribed temperature on the boundary surface Γ_T (*Dirichlet type* boundary conditions). In the latter case, when the heat flux is prescribed on the surface, we have:

$$-k\frac{\partial T}{\partial n} = q_0 \quad \text{on} \quad \Gamma_q \tag{14}$$

where q_0 is the heat flux through the boundary surface Γ_q and $\delta/\delta n$ represents the derivative normal to Γ_q *Neumann type* boundary conditions). Eventually, the specified heat fluxes may be a function of the temperature at the surface as in the case of cooling by radiative emission. The two portion of the boundary surface Γ_T and Γ_q are such that:

$$\Gamma_T \cup \Gamma_q = \Gamma \quad \text{(the whole boundary surface)}$$
$$\Gamma_T \cap \Gamma_q = \theta \quad \text{(the empty set)}$$

Boundary conditions for the transported gas components are specified in a similar way as for the temperature field, and are not described.

Initial conditions

The time integration of the transport equations needs the definition of the initial field of the dependent variables **v**, T, P, and C at time $t = 0$. For consistency, the initial condition must satisfy the transport equations, and in particular the continuity equation. Usually, however, the velocity and pressure field are often initially set to zero. In this case, when there are prescribed non-zero velocity boundary conditions, these initial conditions may be inconsistent with the above equations. This problem is automatically solved by some numerical codes during the first time step by producing a smooth incompressible velocity field which becomes the effective initial condition.

Since the pressure appears into the equations only as the argument of a gradient operator, in the absence of prescribed boundary conditions, the pressure is computed up to an arbitrary constant value and it should be specified in at least one point when absolute values are needed.

TURBULENT TRANSPORT

In the case of laminar flow, fluid velocity follows regular paths and gas particles follow well defined streamlines. However, in the atmosphere this condition is very seldom satisfied and the flow regime is typically turbulent, showing rapid random variations of the velocity field and disallowing the direct solution of the transport equations. To solve this problem, variables are decomposed into their mean values, slowly varying in time, and the fluctuating component describing the rapid, and random, variations (Reynolds decomposition). For the velocity field we have:

$$v_x = \overline{v}_x + v_x' \qquad v_y = \overline{v}_y + v_y' \qquad v_z = \overline{v}_z + v_z' \tag{15}$$

and for the other variables:

$$T = \overline{T} + T'; \qquad C = \overline{C} + C'; \qquad etc. \tag{16}$$

where symbols with over-bar indicate the time averaged values, and symbols with prime represent the random fluctuations overimposed to the mean field:

$$\overline{C} = \frac{1}{\Delta t}\int_t^{t+\Delta t} C dt; \qquad \overline{v}_x = \frac{1}{\Delta t}\int_t^{t+\Delta t} v_x dt; \qquad etc. \tag{17}$$

Δt is the time interval along which the average is performed. Moreover, it is assumed that the mean value of the random fluctuations is null, that is $\overline{T}' = 0$, $\overline{C}' = 0$, $\overline{v}'0$, *etc.* The Reynolds decomposition is based on the possibility to perform the temporal average along time intervals Δt long enough with respect to the time scale of the fluctuations, but short enough with respect to the time scale of the variations of the mean field. In other words, it is assumed that the frequency spectrum of T, C and $\mathbf{v}$ is not null at the low frequencies (mean field), and at the high frequencies (fluctuations), and that these are separated by a frequency gap with null Fourier components.

In the modern approach to the turbulence, the statistical average of any random variable is not performed over a time or space interval, but is considered as the average over a great number of distinct experiments (the statistical ensemble), that is the "mean over all possible states of the system". This change in the definition is based on the assumption that as the averaging interval becomes infinitely great, the time-means converge to the corresponding ensemble means (the ergodic hypothesis) (Monin & Yaglom, 1979).

In the following, we will show how the fluctuating fields generate additional terms into the transport equations, however, for simplicity we will focus on equation (6); being the procedure the same for the momentum and the energy balance equations.After substituting (15) and (16) into (6), and performing the temporal average, we obtain, after manipulation:

$$\frac{\partial \overline{C}}{\partial t} + \frac{\partial(\overline{v}_x \overline{C})}{\partial x} + \frac{\partial(\overline{v}_y \overline{C})}{\partial y} + \frac{\partial(\overline{v}_z \overline{C})}{\partial z} + \frac{\partial \overline{(v_x' C')}}{\partial x} + \frac{\partial \overline{(v_y' C')}}{\partial y} + \frac{\partial \overline{(v_z' C')}}{\partial z} = D\left(\frac{\partial^2 \overline{C}}{\partial x^2} + \frac{\partial^2 \overline{C}}{\partial y^2} + \frac{\partial^2 \overline{C}}{\partial z^2}\right) \tag{18}$$

You may note the presence of additional terms ($\partial(\overline{v'C'})$), representing the divergence of the turbulent fluxes ($\overline{v'C'}$) generated by the fluctuating fields. These terms represent a contribution to diffusion and mixing which may be several orders of magnitude greater than the molecular one.

By applying the Reynolds decomposition to the momentum balance equation for incompressible fluids, in a similar way, we obtain:

$$\rho \frac{\partial \overline{\mathbf{v}}}{\partial t} + \rho \overline{\mathbf{v}} \cdot \nabla \overline{\mathbf{v}} + \rho \nabla \cdot \overline{\mathbf{v}' \mathbf{v}'} = -\nabla \overline{P} + \rho \mathbf{g} + \nabla \cdot \overline{\tau} \tag{19}$$

where use was made of the continuity equation (2). The term $\rho \overline{\mathbf{v}'\mathbf{v}'}$ in the above equation is the Reynolds stress tensor, and represents the additional turbulent flux of momentum due to the random fluctuations. In turbulent flows this term is usually greater than the viscous stress, and the ratio between these two terms is represented by the famous Reynolds number:

$$Re = \frac{\rho U L}{\mu} \tag{20}$$

where U and L are respectively the typical velocity and length scales of the considered problem.

The estimation of the turbulent flux in (18) and the Reynolds stress tensor represents one of the major problems in turbulence theory. Turbulent models should estimate such terms, related to small scale random fluctuations, as a function of the large scale mean field values. In the last century a lot of models were presented by different authors to solve this problem. These models are usually classified as zero-equation models, one-equation models, and two-equation models, depending on the number of partial differential equation used to model the turbulent fluctuations.

In this paper, we will shortly describe the simplest turbulence models, such as K-theory, the Prandtl mixing-length, and a different approach based on the Large Eddy Simulations showing the Smagorinsky model.

K-Theory

K-theory is one of the simplest zero-equation semi-empirical turbulence closure model. It was developed by Boussinesq in 1877, and later proposed by Taylor in 1915 and Schmidt in 1917 (Monin & Yaglom, 1979). It assumes that the turbulent flux of a given variable is proportional to the gradient of its mean value; that is for the generic variable A, transported by the fluid with velocity $\mathbf{v}$:

$$\overline{v_x' A'} = -K_{a,x} \frac{\partial \overline{A}}{\partial x}; \qquad \overline{v_y' A'} = -K_{a,y} \frac{\partial \overline{A}}{\partial y}; \qquad \overline{v_z' A'} = -K_{a,z} \frac{\partial \overline{A}}{\partial z} \tag{21}$$

where $K_{a,x}$, $K_{a,y}$ and $K_{a,z}$ are the eddy diffusion coefficients for the variable A referring to the three spatial dimensions. Eddy diffusion coefficients are in general not constant, being influenced by the atmospheric stability condition, and the presence of the ground boundary. In the case of isotropic turbulence these coefficients are the same. By using (21), with A replaced by C, and substituting into (18), we obtain the following turbulent diffusion equation:

$$\frac{\partial C}{\partial t} + \frac{\partial (v_x C)}{\partial x} + \frac{\partial (v_y C)}{\partial y} + \frac{\partial (v_z C)}{\partial z} = \frac{\partial}{\partial x}\left(K_{C,x} \frac{\partial C}{\partial x} \right) + \\ + \frac{\partial}{\partial y}\left(K_{C,y} \frac{\partial C}{\partial y} \right) + \frac{\partial}{\partial z}\left(K_{C,z} \frac{\partial C}{\partial z} \right) \tag{22}$$

where we have neglected the molecular diffusion compared with the turbulent one and, to simplify the notation, we have dropped the bar sign for the mean fields variables. You may note that this equation has the same structure as (6), where the molecular diffusion coefficients are replaced by the turbulent ones.

In a similar way, K-theory applied to the momentum balance equation give rise to new terms which may be represented by additional contributions to the viscosity coefficient, and the viscosity may be represented as the sum of the molecular viscosity plus the eddy viscosity. At low Reynolds numbers molecular viscosity results greater that the turbulent one, whereas at high Reynolds numbers, molecular viscosity becomes negligible when compared with the turbulent one. In the case of inhomogeneous turbulence, the diffusion coefficients cannot be represented by a single scalar quantity, but need to be represented in a full tensorial form (not shown here).

Mixing-length theory

Mixing-length theory was introduced by Prandtl in 1925. By analogy between the turbulent length scale and the mean free path in the kinetic theory of gases, Prandtl inferred that the Reynolds stress τ_R is proportional to the eddy viscosity ν_T:

$$\tau_R = \rho \nu_T \frac{d\overline{v}}{dz} \tag{23}$$

with

$$\nu_T = l_m^2 \left| \frac{d\overline{v}}{dz} \right| \tag{24}$$

where v is the fluid velocity, and l_m is the mixing-length, which represents the mean distance traveled by a small portion of fluid, before it looses its momentum. Moreover, near a smooth plane boundary, van Kármán (in 1930), and Prandtl (in 1932), using different approaches, obtained the typical relation:

$$l_m = kz \tag{25}$$

where z is the distance from the plane, and κ is the von Kármán constant ($\kappa \approx 0.4$) (Monin & Yaglom, 1979). By using (24) and (25), the Reynolds stress assumes the following form near the wall:

$$|\tau_R| = \rho(\kappa z)^2 \left(\frac{dv}{dz}\right)^2 \tag{26}$$

The integration of the above equation, leads to the so called universal "*law of the wall*", valid for turbulent flows over a smooth plane:

$$v(z) = \frac{v_*}{\kappa} \ln z + \text{const} \tag{27}$$

where $v_* = (\tau T/\rho)^{1/2}$ is the friction velocity.

This law was later extended for rough surfaces, giving the following relation:

$$v(z) = \frac{v_*}{\kappa} \ln\left(\frac{z}{z_0}\right) \tag{28}$$

where z_0 is the roughness length. For completely rough surfaces typically $z_0 = h_0/30$ where h_0 is the mean size of the irregularities of the surface. In the atmospheric boundary layer, these irregularities may have large values as the height of tall grass and trees.

The Smagorinsky model

The Smagorinsky model is particularly suited for numerical algorithms and is often used in "Large-Eddy Simulations" (LES). In the LES the effects of the "large scale" are directly computed, whereas those in the lower scale (the sub-grid scale) are modeled. Since the smaller scale is "more isotropic" than the large scale, the sub-grid-models are more simpler and more universal than those based on the Reynolds stress. The Smagorinsky model is based on the equilibrium between the energy produced at the larger scale and the energy dissipated at the smaller scale, it is assumed that the "eddy viscosity" is given by:

$$\nu_{SGS} = (C_s \Delta)^2 |\bar{S}| \tag{29}$$

where C_s is the Smagorinsky constant, Δ is the filter length scale (proportional to the computational grid), and

$$|\bar{S}| = \sqrt{2\bar{S}_{ij}\bar{S}_{ij}} \quad \text{where} \quad \bar{S}_{ij} \frac{1}{2}\left(\frac{\partial u_i}{\partial x_j} + \frac{\partial u_j}{\partial x_i}\right) \tag{30}$$

and u is the fluid velocity at the "large scale". Smagorinsky model, however, fails in simulating channel flows, overestimating the eddy viscosity by almost an order of magnitude (Ferziger & Peric, 1999). In the regions near the surfaces of the channel, a further reduction of the mixing length scale is often modeled by introducing the van Driest damping function (van Driest, 1956):

$$C_s = C_{so}(1 - e^{-z_*/A}) \tag{31}$$

where A is a constant usually taken to be approximately 25, and z_* is the adimensional distance from the wall:

$$z_* = \frac{z u_*}{\nu} \tag{32}$$

where z is the distance from the wall, ν is the kinematic viscosity, v_* is the shear velocity ($\nu_x = \sqrt{\tau_w / \rho}$ where τ_w is the shear stress at the wall).

NUMERICAL SOLUTION OF THE TRANSPORT EQUATIONS

Transport equations contain non-linear terms, and are often difficult to solve analytically (if not impossible). Analytical solutions exist only for a limited set of problems with simple geometries and boundary conditions. In most practical cases a numerical solution is needed. Numerical solutions, however, are only discrete approximations of the solution of the partial differential equations, defined in the continuum, and are affected by truncation and round-off errors. The former are intrinsic in the discretization algorithm, whereas the latter depend on the precision of the utilized computational machine, and are partially controlled by the numerical procedure. Numerical schemes for the solution of the transport equations are based on the discretization of the field variables (velocity, pressure, temperature, *etc.*) on a spatial grid, and often the partial derivatives are approximated by the corresponding finite difference (Finite Difference method), transforming the partial differential equations into a non-linear system of algebraic equations. As will be described in the next section, the Finite Element method uses a different approach for transforming the problem into the system of algebraic equations, and can be considered a more general technique for the solution of partial differential equations, including the Finite Difference method as a particular case [Zienkiewicz & Taylor, 1991]. Moreover, time-dependent problems need a further integration in time, and are often based on classical time-marching algorithms. These can be *explicit* when the discretized time derivative of a given variable is represented directly as a function of the variables computed at the current time step, or *implicit*, when they contain a reference to values that still need to be computed. This last scheme is generally more stable than the previous one, but needs more computational efforts, and often adopts iterative techniques.

The Finite Element Method

In this brief discussion we will focus on the Finite Element Method for the solution of the transport equations. The existing literature on the subject is huge, and a lot of computer codes are available for the solution of the transport equations based on this technique. A complete review on the method is out of the scope of this paper, and we will just illustrate the major problems encountered in the solution of the transport equations for incompressible fluids with the finite element method, restricting to a particular algorithm: the Petrov-Galerkin scheme.

The physical domain of interest Ω is divided into a complete set of N_e disjoint elements Ω^e covering the whole domain:

$$\Omega = \bigcup_{e=1}^{Ne} \Omega^e; \qquad \Omega^{e1} \bigcap \Omega^{e2} = \theta \quad (e_1 \neq e_2) \tag{33}$$

These elements may have different shapes, such as triangles, quadrilaters, tetrahedrons, cubes, *etc.* Inside each element Ω^e the field variables are approximated by a linear combination of the values defined at the nodes α of the element:

$$v_i(x,y,z,t) = \sum_{\alpha} N^v_{\alpha}(x,y,z) v_{\alpha,i}(t) \tag{34}$$

where v_i is the *i–th* component of the velocity, $v_{\alpha,i}$ is the value of the velocity component i defined at node α of the element, N^v_{α} are the interpolating polynomial functions (the shape functions) for the velocity field defined inside the element, and the sum is extended over the nodes belonging to the considered element. The shape functions referring to each node are defined only inside the corresponding element and are null outside; moreover they are usually chosen in such a way that the resulting velocity field is continuous across the elements boundaries. The whole velocity field is obtained as a piecewise polynomial field obtained by merging the elements. In a similar way, the pressure field is approximated by:

$$P(x,y,z,t) = \sum_{\beta} N^p_{\beta}(x,y,z) P_{\beta}(t) \tag{35}$$

where P_{β} are the nodal values of the pressure field, and $N_{p\beta}$ are the shape functions for the pressure field. In the case of incompressible fluids, to avoid the well known effect of "locking", the degree of the interpolating polynomial used to interpolate the pressure field is chosen smaller (by one degree) than that of the velocity field. Moreover, the pressure nodes not necessarily coincide with the element nodes in which the velocity field is defined.

As an example, we consider rectangular two-dimensional elements. We define the two components of the velocity field at the four nodes of the quadrilateral, with bi-linear interpolation inside the element (polynomial of degree one). The pressure field is constant inside the element (polynomial of degree zero), and is defined at the element center. At the four nodes where the velocity field is defined, are associated four shape functions each characterized by the value *one* at the corresponding node, a *null* value at the other three nodes, and a value between zero and one inside the element, obtained by a bi-linear interpolation. However, the chose of the element shapes, and the interpolating polynomial is not arbitrary, but should satisfy particular conditions (eg: Babuska-Brezzi criterion, *etc.*) [Zienkiewicz & Taylor, 1991].

The resulting velocity and pressure fields are an approximation of the solution of eq.(2) and eq. (3), and cannot satisfy them exactly. To find the nodal values of the velocity and pressure fields, equations (2) and (3) are replaced by their weak forms:

$$\int_{\Omega} w_1(\nabla \cdot \mathbf{v})d\Omega = 0 \tag{36}$$

$$\int_{\Omega} w_2\left(\frac{\partial}{\partial t}(\rho \mathbf{v}) + \nabla \cdot (\rho \mathbf{v}\mathbf{v}) + \nabla P - \rho \mathbf{g} - \nabla \cdot \tau\right)d\Omega = 0 \tag{37}$$

$$\int_{\Omega} w_3\left[\rho c_p\left(\frac{\partial T}{\partial t} + \mathbf{v} \cdot \nabla T\right) - \nabla \cdot (k\nabla T) - \tau : \nabla \mathbf{v}\right]d\Omega = 0 \tag{38}$$

where Ω represents the physical domain defining the system of interest, and $w1$, w_2 and w_3 are arbitrary weighting functions. In a similar way, (22) is written in the weak form. It is obvious that when (2), (3), (5) and (22) are satisfied, also the corresponding weak forms are satisfied; whereas the reverse is not necessarily true. In the Finite Element method (weighted residual approach) it is required that the approximated velocity and pressure fields obtained by (34) and (35), satisfy the weak form of the transport equations. After substitution of (34) and (35) into (36) and (37), these last equations transform into a non-linear system of algebraic equations where the nodal values of the velocity and pressure are the unknowns (when not already defined at the boundaries).

A particular role is played by the arbitrary weighting functions and which are often chosen in order to optimize the numerical algorithm. According to the Galerkin scheme, the weighting functions are chosen equivalent to the shape functions of the velocity field. However, this choice results in numerical instabilities in the case of convection dominated flows when the Reynolds number is greater than one (Peclet number for the enthalpy equation). For such regimes, the Petrov-Galerkin formulation is adopted. The new weighting functions w are obtained by adding a supplemental asymmetric upwinding term s to the Galerkin weighting functions (Hughes et al., 1979; Brook & Hughes, 1982; Zienkiewicz & Taylor, 1991):

$$\overline{w} = w + \overline{s} \tag{39}$$

where s is a function of the local Reynolds number. An alternative method, known as the Least Square-Galerkin approximation, is also used to avoid instabilities (Zienkiewicz & Taylor, 1991).

After integration, usually performed numerically using Gauss quadrature, equations (36) and (37) yield to a set of algebraic equations which may be written in matricial form as:

$$\mathbf{M}\boldsymbol{a} + \mathbf{C}\boldsymbol{v} + \mathbf{N}(\boldsymbol{v}) - \mathbf{G}\boldsymbol{P} = \mathbf{F} \tag{40}$$

$$\mathbf{G}^{\mathrm{T}}{}_{\mathrm{v}} = \mathbf{D} \tag{41}$$

In the above equations, vector $\boldsymbol{v}$ represents the nodal values of the velocity v_i, whereas vector $\boldsymbol{a}$ represents the nodal values of the time derivatives of the velocity v_i. $\boldsymbol{P}$ represents the pressure field; M is the consistent generalized mass matrix; $\mathbf{C}$ and $\boldsymbol{N}(\boldsymbol{v})$ account respectively for the diffusive and the nonlinear convective terms. $\boldsymbol{F}$ is a generalized force vector. The weak forms of the energy equation (5) and the gas diffusion equation (22) are built in a similar way. In eq. (41), $\boldsymbol{D}$ accounts for the prescribed boundary velocity on the continuity equation, and $\boldsymbol{G}$ is the gradient operator. This system of (nonlinear) algebraic equations is often solved by direct methods when the number of elements is not too big, otherwise iterative methods are used. Time integration is performed by the standard explicit (eg: Euler method) or implicit methods (eg: predictor-corrector, Crank-Nicholson, *etc.*).

EXAMPLE

In this section two examples of atmospheric dispersion of a pollutant gas (CO_2) emitted from the ground are shown. For simplicity we assume that the physical domain is two-dimensional (in the plane x-z), and infinite in the transversal direction (y). We consider a space domain 20 m long in the horizontal direction (x axis) and 2 m high (along z axis). CO_2 is emitted from a small area 2 m wide, with vertical velocity $v_{z,0} = 0.03$ m/s, and T_{CO2}, and the surrounding atmosphere is initially at $T_a = 20°C$ (a typical situation in high CO_2 emission vents in Italy (Rogie et al., 2000)). A no-slip condition $\mathbf{v} = 0$, is assumed at the lower boundary (ground) except in the emission area, where the velocity is $\mathbf{v} = (0, v_z)$. Wind is assumed null in the first example, whereas, in the second case, it is described by a logarithmic profile along x axis, described by eq. (28) with $z_0 = 0.1$ m, and $v_x = 5$ m/s at 10m of altitude. A free-flow condition is specified at the upper and right boundaries, and a fixed wind velocity (null in the first example) is assumed at the left boundary. Gas dispersion is modeled as an incompressible fluid, in the Boussinesq approximation; that is the difference of densities is accounted for only in the body force term of the momentum equation (3), which becomes:

$$\rho_0\left(\frac{\partial \mathbf{v}}{\partial t} + \mathbf{v}\cdot\nabla\mathbf{v}\right) = -\nabla P + \rho\mathbf{g} + \nabla\cdot\tau \tag{42}$$

where ρ_0 is the reference density, taken here equal to the initial air density. A parameter (C), ranging between zero and one describes the CO_2 mass fraction:

$$C = \frac{\text{mass of } CO_2}{\text{mass of air } + \text{ mass of } CO_2} \tag{43}$$

The total gas density ρ can be expressed as a function of the pure CO_2 and air densities ρ_{co_2} and ρ_a by:

$$\frac{1}{\rho} = \frac{C}{\rho_{co_2}} + \frac{1-C}{\rho_a} \tag{44}$$

Under the assumption that both air and CO_2 behave like the perfect gas, we have:

$$\rho_{co_2} = \frac{PM_{co_2}}{RT}; \quad \rho_a = \frac{PM_a}{RT}; \quad \frac{1}{\rho} = \frac{RT}{P}\left(\frac{C}{M_{co_2}} + \frac{1-C}{M_a}\right) \tag{45}$$

where P is the pressure, R is the universal gas constant ($R = 8.314$ J K^{-1}mole^{-1}), and M_{co2} (44 g/mole) and M_a (29 g/mole) are respectively the molecular weights of CO_2 and air. By assuming that heat exchange due to air and CO_2 mixing is more efficient than heat transfer by conduction, and that the eddy diffusion coefficients for the temperature are equal to the eddy diffusion coefficients of the CO_2 molecules (mass and heat diffuse together), we may express the mixing temperature T in the above equation as a function of the initial CO_2 and air temperatures T_{co2} and T_a, without the need of solving the energy equation (5):

$$T = \frac{C_{Cp,co_2}T_{co_2} + (1-C)_{Cp,a}T_a}{C_{Cp,co_2} + (1-C)_{Cp,a}} \tag{46}$$

where $c_{p,co2}$ (= 845 J Kg^{-1}K^{-1}) and $c_{p,a}$ (= 1005 J Kg^{-1}K^{-1}) are respectively the heat capacities at constant pressure of the CO_2 and air.

Equations (2), (22) and (42) are solved using the Finite Element method using the Petrov-Galerkin scheme. Fig. 1 shows the initial velocity distribution of the gas. CO_2 is emitted from below, and wind is null. Dots represent the nodes of the 800 elements (40 x 20) used to discretize the interested domain. Turbulence is accounted for with the Smagorinsky model. After 4 s, (see Fig. 2) CO_2 fills part of the lower domain, and spreads horizontally because of its greater density that the surrounding air. Fig. 3 shows the CO_2 concentration after 40 s. In the second example, gas is emitted in the atmosphere in the presence of a horizontal wind blowing from left to right, with a logarithmic velocity profile ranging from zero at the lower boundary, to about 3m/s at the upper boundary (2 m high). Fig. 4 shows the gas concentration after 4 s, whereas Fig. 5 shows the gas concentration after 40 s.

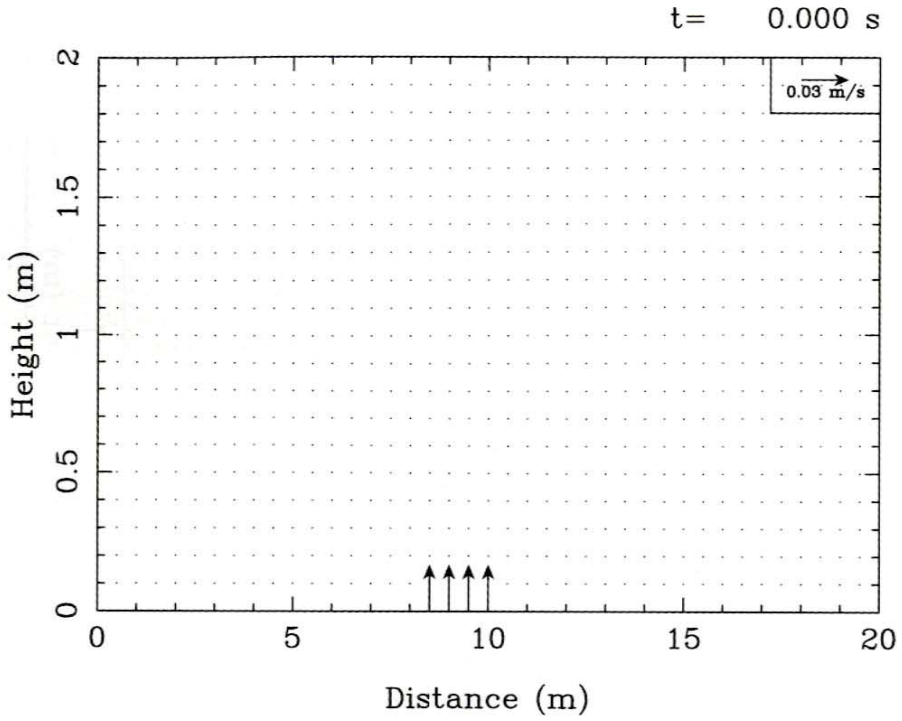

Figure 1. Initial velocity distribution of CO_2 in the considered domain. Horizontal wind is null. Please note that the vertical scale is different from the horizontal one.

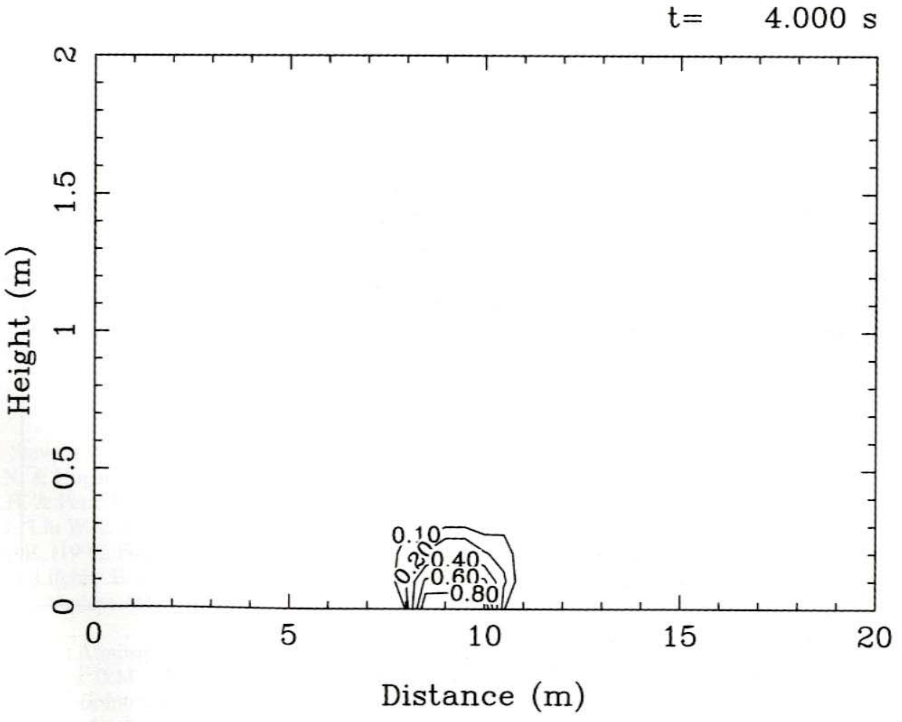

Figure 2. CO_2 concentration after 4 s from the beginning of the emission. Horizontal wind has a logarithmic profile.

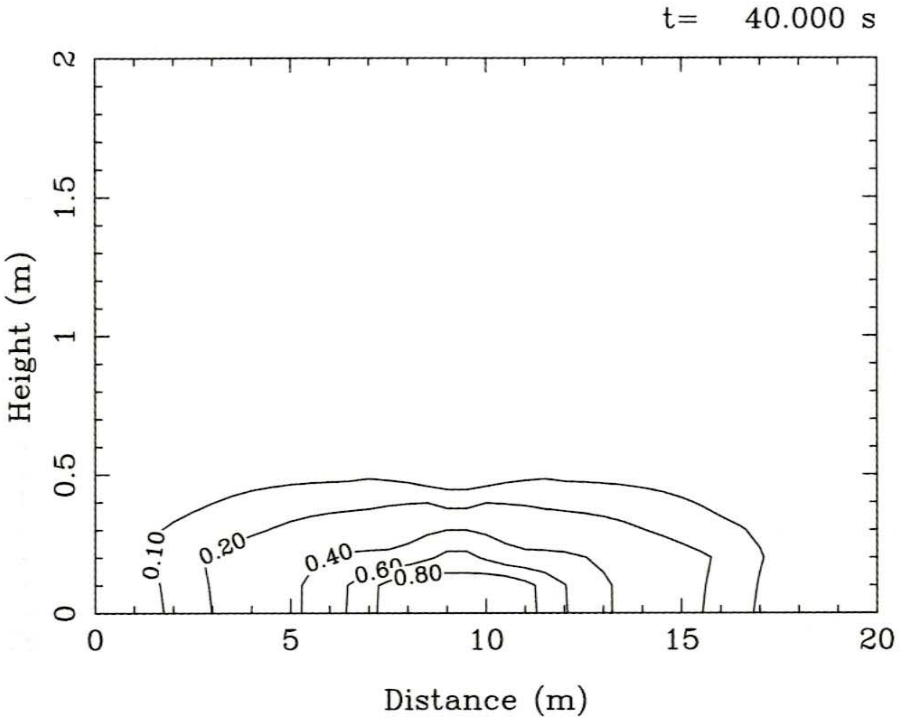

Figure 3. CO_2 concentration after 40 s from the beginning of the emission. Horizontal wind is null.

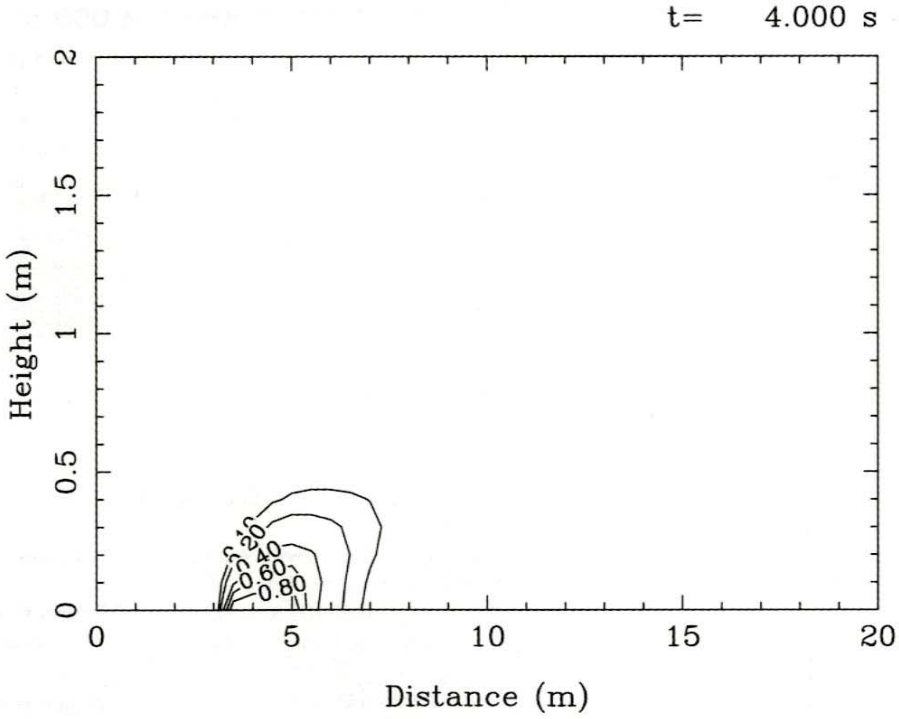

Figure 4. CO_2 concentration after 4 s from the beginning of the emission. Horizontal wind has a logarithmic profile.

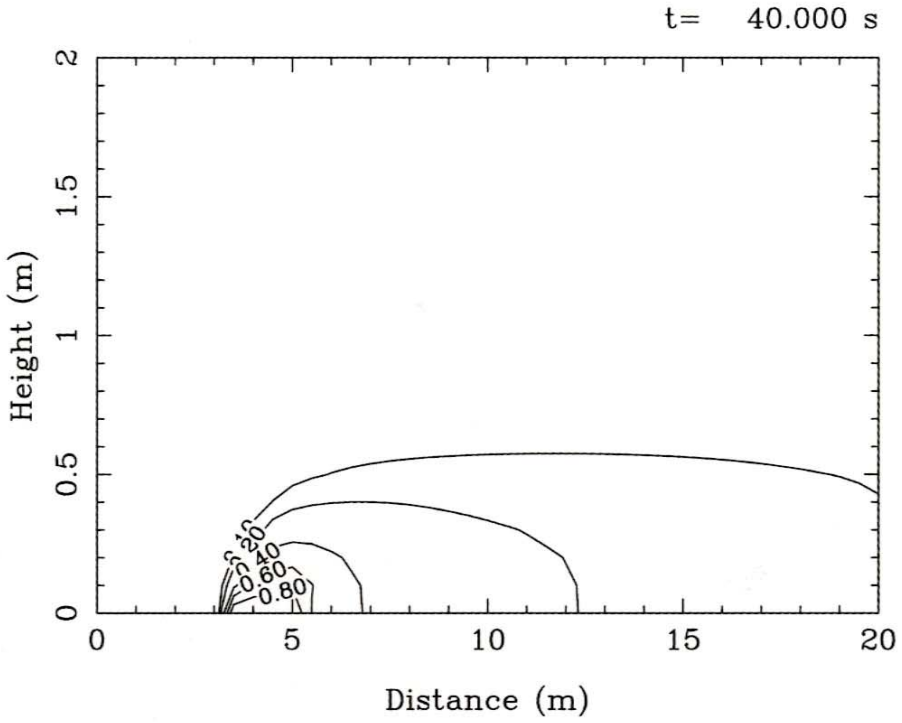

Figure 5. CO_2 concentration after 40 s from the beginning of the emission. Horizontal wind has a logarithmic profile

CONCLUSIONS

This paper shortly illustrates the basic equations of the transport theory of incompressible fluids, and the application of the Finite Element Method to the solution of a simple problem of gas diffusion from a ground source in 2-D, although a realistic description of the turbulence needs a 3-D model. This method can also be used in the case of a more complex topography. Considerations on the atmosphere stability are not discussed in the text, and models assume stable atmospheric conditions. Obviously, the presence of a particular thermal gradient in the atmosphere, or the immission of warmer gases could lead to the formation of buoyant plumes. Turbulence plays an important role in atmospheric processes, and must be considered in numerical codes. Zero-equation models for turbulence closure, although less accurate than higher order models, provide an easy way to account for turbulence. In this paper, the important role played by solar heating and the presence of water vapour in the atmosphere was not considered for simplicity; however, these effects should be included in realistic models.

REFERENCES

Bird R.B., Stewart W.E. & Lightfoot E.N. (1960) Transport Phenomena, Wiley and Sons, New York.
Brooks A.N. & Hughes T.J.R. (1982) *Comput. Methods Appl. Mech. Engrg.*, 32, 199-259.
Ferziger J.H. & Peric M. (1999) Computational Methods for Fluid Dynamics, Springer Verlag.
Hughes T.J., Liu W.K. & Brooks A. (1979) *J. Comput. Phys.*, 30, 1-60.
Jacobson M.Z. (1999) Fundamentals of atmospheric modelling, Cambridge University Press, United Kingdom.
Landau L. & Lifchitz E. (1971) Mécanique des Fluides, vol. VI, MIR, Moscow, URSS.
Monin A.S. & Yaglom A.M. (1979) Statistical Fluid Mechanics: Mechanics of Turbulence, The MIT Press, USA, Volumes 1 and 2.
Pasquill F. (1974) Atmospheric Diffusion, John Wiley & Sons, Chichester, England, 2nd edition.
Rogie J.D., Kerrick D.M., Chiodini G. & Frondini F. (2000) *J. Geophys. Res.*, 105(B4), 8435-8445.
Stull R.B. (1988) An Introduction to Boundary Layer Meteorology, Kluwer Academic Publisher, Dordrecht, The Netherlands.
van Driest E.R. (1956) *J. Aero. Sci.*, 23, 1007-1011.
Zienkiewicz O.C. & Taylor R.L. (1991) The Finite Element Method, McGraw Hill, 4th edn., Volumes 1 and 2.